COMPUTER VISION, GRAPHICS, AND IMAGE PROCESSING 41, 57–79 (1988)

Wavelength Selection for Synthetic Image Generation

GARY W. MEYER*

Program of Computer Graphics, Cornell University, Ithaca, New York

Received June 22, 1986; accepted July 20, 1987

The efficient synthesis of color in computer graphics is dependent on modelling the correct number and spacing of wavelengths across the visible spectrum. It has recently been shown that the opponent representation of the fundamental spectral sensitivity functions is optimal from the point of view of statistical communication theory. This result is used in this paper to guide the selection of wavelengths for synthetic image generation. Gaussian quadrature with the opponent fundamentals as weighting functions is used to choose the wavelengths. This approach is shown to be superior to using Gaussian quadrature with the fundamental spectral sensitivity functions or the CIE *XYZ* matching functions. The technique is evaluated by using color difference calculations and by comparisons between a real scene and a computer generated picture of that scene.

1. INTRODUCTION

Sophisticated lighting models employed in computer graphics today synthesize color by computing spectral energy distributions on a wavelength by wavelength basis (Cook and Torrance [1], Hall and Greenberg [2]). Reflectances are assigned to materials, emittances are associated with light sources, and models of how light interacts with matter are used to determine the spectral energy distributions that would reach an observer of the scene. These spectral energy distributions are converted to tristimulus values by using the principles of color science. Finally, these color coordinates are transformed into a set of tristimulus values appropriate for a particular color reproduction device.

There are several objectives to be met in performing these calculations. Although any linear transform of the human spectral sensitivities defines a valid color space in which to represent the tristimulus values, a color space should be chosen which minimizes any errors that might be inherent in the computations. Furthermore, since the lighting model calculations may have to be repeated for every wavelength used, the minimum number of wavelengths necessary to ensure adequate color fidelity should be employed to represent the spectral energy distribution. In addition, the wavelengths used should be spaced across the visible spectrum so that they are located at the positions most important for accurate color rendition.

This paper shows how gaussian quadrature with a set of opponent fundamentals can be used to select the wavelengths at which to perform synthetic image generation. First a set of opponent fundamentals are derived from the CIE *XYZ* matching functions and are shown to be the basis for an optimal color space in which to perform color synthesis calculations. Next the wavelengths at which to conduct realistic image synthesis are selected via gaussian quadrature with the opponent fundamentals as weighting functions. Finally, this wavelength selection technique is

*Present address: Department of Computer and Information Science, University of Oregon, Eugene, Oregon 97403.

0734-189X/88 $3.00

evaluated by color difference calculations on a set of representative spectral energy distributions and by a perceptual comparison experiment between a real scene and a computer generated picture of that scene.

2. AN OPTIMAL COLOR SPACE FOR COLOR SYNTHESIS

The color space that is employed for color synthesis work should be selected so as to minimize any errors inherent in the computation. The fundamental spectral sensitivity functions of the human visual system are what all color reproduction techniques are based upon. They are introduced in the following subsection. However, the color space that is formed by the fundamental spectral sensitivity functions is not optimal from the standpoint of color synthesis work. In the second subsection, the results of Buchsbaum and Gottschalk [3] are used to derive an opponent representation of these fundamentals by the use of the Karhunen–Loeve expansion. The color space that results from this transformation minimizes the error of representation for the tristimulus values and hence reduces the errors that occur in color synthesis calculations.

2.1. The Fundamental Spectral Sensitivities

The fundamental spectral sensitivities of the human visual system form the basis for any color calculations in realistic image synthesis. Given the 1931 CIE standard observer matching functions ($\bar{x}(\lambda)$, $\bar{y}(\lambda)$, and $\bar{z}(\lambda)$), a set of dichromatic confusion loci, and a method for establishing the relative sensitivity of the resulting functions, the following definition of the fundamental spectral sensitivities (Fig. 1) can be

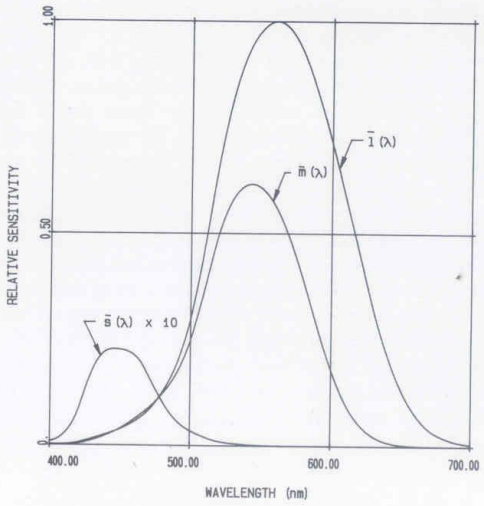

FIG. 1. The fundamental spectral sensitivity functions.

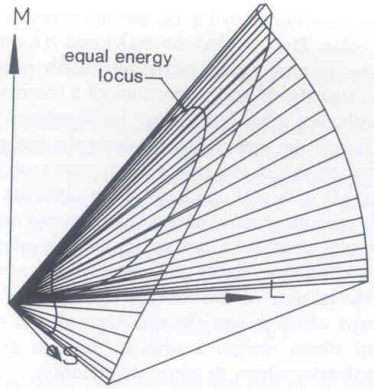

FIG. 2. Equal energy spectrum locus and cone of realizable color in *SML* space. spectral sensitivities were all normalized to 1.0 to plot the equal energy spectrum locus.)

derived

$$\begin{bmatrix} \bar{s}(\lambda) \\ \bar{m}(\lambda) \\ \bar{l}(\lambda) \end{bmatrix} = \begin{bmatrix} 0.0000 & 0.0000 & 0.0127 \\ -0.2606 & 0.7227 & 0.0562 \\ 0.1150 & 0.9364 & -0.0203 \end{bmatrix} \begin{bmatrix} \bar{x}(\lambda) \\ \bar{y}(\lambda) \\ \bar{z}(\lambda) \end{bmatrix}.$$

The details of this derivation can be found in Appendix A. The S, tristimulus values are determined for a spectral energy distribution $E(\lambda)$

$$S = \int_{380}^{770} E(\lambda)\bar{s}(\lambda)\, d\lambda$$

$$M = \int_{380}^{770} E(\lambda)\bar{m}(\lambda)\, d\lambda$$

$$L = \int_{380}^{770} E(\lambda)\bar{l}(\lambda)\, d\lambda,$$

where 380 nm and 770 nm are taken as the limits of the visible spectr paper. Figure 2 shows an *SML* coordinate system and the cone of realiz that forms the boundary of all possible tristimulus values.

2.2. The Opponent Spectral Sensitivities

In order to minimize the effect of any errors that might happen while sy colors, the axes of the color space which is used to perform the calculatic be oriented so that they pass through the regions where tristimulus value likely to occur. In addition to being limited to a particular region of color

the cone of realizable color. The fact that the $\bar{m}(\lambda)$ and $\bar{l}(\lambda)$ spectral sensitivities in Fig. 1 overlap each other to such a great extent but hardly overlap the $\bar{s}(\lambda)$ spectral sensitivity at all means that the M and L portions of a tristimulus value will always be highly correlated with each other but will not be correlated with the S portion of a tristimulus value. This can be seen in Fig. 2 where the locus for the equal energy spectral energy distribution makes two major loops: one loop in the LM plane at a 45° angle to the L and M axes and one loop in the direction of the S axis. If it is assumed that relatively smooth spectral energy distributions are more likely to occur than spikey spectral energy distributions, then tristimulus values at the boundary of the cone where monochromatic lights are represented are less probable than tristimulus values in the interior of the cone. A transform of the SML coordinate system should be sought which directs the axes through the most dense regions of tristimulus values and which assigns a priority to each axis depending on the proportion of the coordinates which lie along its direction.

The discrete Karhunen–Loeve expansion can be used to find such a transform. The application of this technique to the study of human color vision was first performed by Buchsbaum and Gottschalk [3, 4]. The new coordinates A, C_1, and C_2 which result from the transformation

$$\begin{bmatrix} A \\ C_1 \\ C_2 \end{bmatrix} = \begin{bmatrix} & T & \end{bmatrix} \begin{bmatrix} S \\ M \\ L \end{bmatrix} \tag{3}$$

should be prioritized in such a way that they can be distorted or even eliminated one by one with minimum impact on the mean squared error. It can be shown [5] that this will happen when the rows of the transformation matrix T are the eigenvectors of the covariance matrix

$$\begin{bmatrix} C_{SS} & C_{SM} & C_{SL} \\ C_{SM} & C_{MM} & C_{ML} \\ C_{SL} & C_{ML} & C_{LL} \end{bmatrix} \tag{4}$$

where

$$\begin{aligned} C_{SS} &= \int\int K(\lambda,\mu)\bar{s}(\lambda)\bar{s}(\mu)\,d\lambda\,d\mu \\ C_{SM} &= \int\int K(\lambda,\mu)\bar{s}(\lambda)\bar{m}(\mu)\,d\lambda\,d\mu \end{aligned} \tag{5}$$

with similar expressions for the other terms. $K(\lambda,\mu)$ is the covariance function and $\bar{s}(\lambda)$, $\bar{m}(\lambda)$, and $\bar{l}(\lambda)$ are the fundamental spectral sensitivities defined in Eq. (1). The eigenvalue for each eigenvector determines the amount by which the mean squared error increases when the corresponding coordinate is deleted. This can be used to assign a relative importance to each coordinate.

$$K(\lambda,\mu) = E\{P(\lambda)P(\mu)\} - E\{P(\lambda)\}E\{P(\mu)\},$$

where $E\{\ \}$ is the expectation operator and $P(\lambda)$ is an arbitrary member of t of spectral energy distributions $[P(\lambda)]$. If the correlation between individual lengths is assumed to be so small that spectral energy distributions which con a spike at a single wavelength are possible, then the Fourier frequency spectrum for the set $[P(\lambda)]$ must contain uniform energy at all freque $K(\lambda,\mu)$, which is the Fourier transform of the frequency power spectrum [6 then have the value

$$K(\lambda,\mu) = \delta(\lambda-\mu)$$

where $\delta(\ )$ is the dirac delta function and the energy at each frequency has normalized to 1.0. This leads to

$$\begin{aligned} C_{SS} &= \int \bar{s}(\lambda)\bar{s}(\lambda)\,d\lambda & C_{SM} &= \int \bar{s}(\lambda)\bar{m}(\lambda)\,d\lambda \\ C_{MM} &= \int \bar{m}(\lambda)\bar{m}(\lambda)\,d\lambda & C_{SL} &= \int \bar{s}(\lambda)\bar{l}(\lambda)\,d\lambda \\ C_{LL} &= \int \bar{l}(\lambda)\bar{l}(\lambda)\,d\lambda & C_{ML} &= \int \bar{m}(\lambda)\bar{l}(\lambda)\,d\lambda. \end{aligned}$$

Note that since the wavelengths of the spectral energy distributions in the set [were modelled as being minimally correlated, it is only the correlation betwe fundamental spectral sensitivities which is incorporated into the covariance n

Substituting the fundamental spectral sensitivities as defined in Eq. (1) in (8), forming the transformation matrix in Eq. (3) from the eigenvectors covariance matrix in Eq. (4), and concatenating the matrices in Eqs. (1) a leads to the following transformation from 1931 CIE XYZ space to the o AC_1C_2 space:

$$\begin{bmatrix} A \\ C_1 \\ C_2 \end{bmatrix} = \begin{bmatrix} -0.0177 & 1.0090 & 0.0073 \\ -1.5370 & 1.0821 & 0.3209 \\ 0.1946 & -0.2045 & 0.5264 \end{bmatrix} \begin{bmatrix} X \\ Y \\ Z \end{bmatrix}.$$

The eigenvalue ratio is

$$102.4 : 2.29 : 0.0221$$

between A, C_1, and C_2, respectively.

The prioritization of the coordinates indicated in Eq. (10) can be se comparing Fig. 3 of the new AC_1C_2 space with Fig. 2 of SML space. The A roughly positioned along the line that lies at 45° with respect to the L and M and thus passes through the most dense region of tristimulus values. This is b

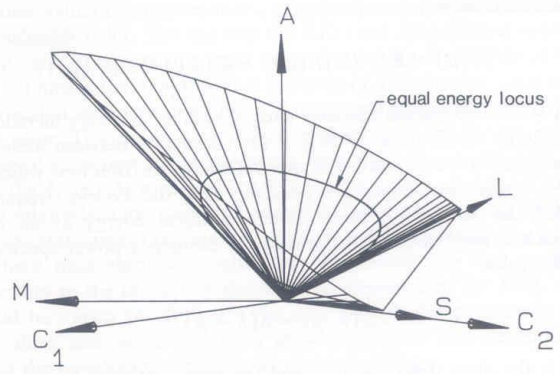

FIG. 3. Equal energy spectrum locus, SML axes, and cone of realizable color in AC_1C_2 space.

of the high correlation between the L and M components of the tristimulus value Although it is difficult to see in Fig. 3, the C_1 axis lies in the LM plane. Since it perpendicular to the A axis which points in the direction of high L and component correlation, the C_1 axis records the differences between the L and components of the tristimulus values. The C_2 axis lies close to the S axis and th primarily records the value of the relatively insensitive short wavelength receptor.

The $\bar{a}(\lambda)$, $\bar{c}_1(\lambda)$, and $\bar{c}_2(\lambda)$ sensitivities which correspond to the A, C_1, and coordinates are shown in Fig. 4. They are very similar in shape to many of t opponents fundamentals which have been proposed for the human visual syste The achromatic channel, designated as A, corresponds closely to the photop luminous efficiency function $\bar{y}(\lambda)$. The chromatic channels, designated as C_1 a C_2, correspond to the red/green and yellow/blue functions of the classical opp nent fundamentals. Buchsbaum and Gottschalk [3] were able to directly compa their fundamentals to those of Ingling [7] and Guth *et al.* [8] because all thr studies used the 1951 Judd modified matching functions. This comparison yield excellent results.

3. COMPUTING TRISTIMULUS VALUES VIA GAUSSIAN QUADRATURE

Given the optimal AC_1C_2 color space in which to conduct color synthes attention will now be turned to the evaluation of the integrals

$$A = \int E(\lambda)\bar{a}(\lambda)\,d\lambda$$

$$C_1 = \int E(\lambda)\bar{c}_1(\lambda)\,d\lambda \qquad (1$$

$$C_2 = \int E(\lambda)\bar{c}_2(\lambda)\,d\lambda.$$

A quadrature technique is sought that will achieve high accuracy for few wa lengths and that can take advantage of the shape of the $\bar{a}(\lambda)$, $\bar{c}_1(\lambda)$, and $\bar{c}_2($

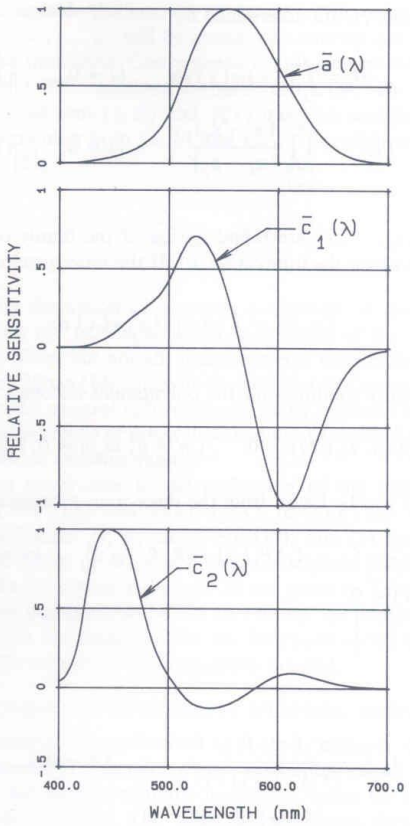

FIG. 4. Spectral sensitivities for AC_1C_2 space.

spectral sensitivities to position these wavelengths at the best locations in the spectrum. Gaussian quadrature, which incorporates the notion of a weighting function in its definition, is the clear choice for this problem. Although it is analytically defined for only a small set of classical weighting functions, gaussian quadrature can be used with an arbitrary weighting function by employing numerical techniques. Wallis [9] and MacAdam [10] have applied the technique to the computation of tristimulus values from the 1931 CIE XYZ matching functions.

Given a function $f(x)$, a weighting function $w(x)$, and an interval (a, b), the gaussian rules for integration are [11]

$$\int_a^b f(x)w(x)\,dx \simeq \sum_{i=0}^{n} H_i f(x_i), \tag{12}$$

where the coefficients H_i are determined by

$$H_i = \int_a^b l_i(x)w(x)\,dx \qquad (i = 0, \ldots, n)$$

$$l_i(x) = \prod_{\substack{j=0 \\ j \neq i}}^{n} \frac{(x - x_j)}{(x_i - x_j)} \qquad (i = 0, \ldots, n). \tag{13}$$

The abscissas $x_0, x_1, \ldots, x_n$ are found by use of the family of polynomials $P_n(x)$ orthogonal to $w(x)$ over the interval (a, b). If the inner product is defined as

$$\langle g, h \rangle = \int_a^b g(x)h(x)w(x)\,dx \tag{14}$$

then the orthogonality condition for the polynomials becomes

$$\langle P_n(x), P_m(x) \rangle = 0 \qquad (m \neq n;\ m, n = 0, 1, 2, \ldots). \tag{15}$$

These polynomials can be found from the three term recurrence relation [12]

$$\begin{aligned} P_{k+1}(x) &= (x - A_k)P_k(x) - B_k P_{k-1}(x) \qquad (k = 0, 1, \ldots) \\ P_{-1}(x) &= 0 \\ P_0(x) &= 1, \end{aligned} \tag{16a}$$

where

$$\begin{aligned} A_k &= \frac{\langle xP_k(x), P_k(x) \rangle}{\langle P_k(x), P_k(x) \rangle} \qquad (k = 0, 1, \ldots) \\ B_k &= \frac{\langle P_k(x), P_k(x) \rangle}{\langle P_{k-1}(x), P_{k-1}(x) \rangle} \qquad (k = 1, 2, \ldots). \end{aligned} \tag{16b}$$

The abscissas $x_0, x_1, \ldots, x_n$ are the zeros of the $n + 1$ order orthogonal polynomia defined above.

If $w(x)$ is nonnegative on (a, b), gaussian quadrature can be shown to hav several important convergence and error properties. For $f(x)$ a polynomial o degree less than or equal to $2n + 1$, Eq. (12) is exact. If $f(x)$ is not such polynomial but is still continuous on (a, b) (or even discontinuous in certain case convergence is guaranteed in the limit as n goes to infinity [13]. In terms of erro estimates, gaussian quadrature can be shown to be as good as any other quadratur formula that employs the same number of points [13]. This property is not affecte by integrals which only have low order derivatives.

Many of the desirable properties of gaussian quadrature continue to hold if $w(x$ assumes negative values on (a, b). The existence of the orthogonal polynomia $P_n(x)$ does not depend on the nonnegativity of $w(x)$, but some of the zeros of the

polynomials may lie outside the interval (a, b) [13]. This means that some of the integration points $x_0, x_1, \ldots, x_n$ will lie outside the interval and that certain orders of integration will be undefined. Convergence is still guaranteed when $w(x)$ takes on negative values but the conditions are more restrictive. The integration points must lie in a bound segment (c, d) and $f(x)$ must be continuous in (α, β), the smallest segment containing both (a, b) and (c, d). In addition, there must be a number K such that [13]

$$\sum_{i=0}^{n} |H_i| \leq K. \tag{17}$$

Given the preceeding discussion of gaussian quadrature, it can be seen that the feasibility of applying the technique to the calculation of the AC_1C_2 tristimulus values is quite good. Most, but not all, spectral energy distributions are continuous. This was indicated by Moon [14] where he showed that low order polynomials could be used to represent the spectral reflectances of many common materials. The only limitation is that certain orders of integration will not be defined due to the fact that $\bar{c}_1(\lambda)$, and $\bar{c}_2(\lambda)$ take on negative values.

To apply gaussian quadrature to the evaluation of the integrals in Eq. (11): (1) substitute $E(\lambda)$ for $f(x)$ and $\bar{a}(\lambda)$, $\bar{c}_1(\lambda)$, or $\bar{c}_2(\lambda)$ for $w(x)$ in Eq. (11); (2) compute the coefficients H_i by using Eq. (13); and (3) find the wavelengths $\lambda_0, \lambda_1, \ldots, \lambda_n$ as the zeroes of the $n + 1$ order orthogonal polynomials defined in Eq. (16a). The results for orders 1 through 10 are given in Tables 1a and 1b. The interval of integration was taken to be 380 to 770 nm. As predicted, certain orders of gaussian quadrature are undefined for the functions $\bar{c}_1(\lambda)$ and $\bar{c}_2(\lambda)$ because they yield wavelengths outside of the integration interval.

4. EVALUATION OF WAVELENGTH SELECTION TECHNIQUE

A series of experiments was performed in order to evaluate the effectiveness of using gaussian quadrature to determine AC_1C_2 tristimulus values. In one set of tests, gaussian quadrature was used to compute tristimulus values for a representative set of spectral energy distributions. The color difference was then determined in a perceptually uniform color space between the actual and the computed tristimulus values for these spectral energy distributions. In another set of tests, gaussian quadrature was used to produce several computer generated pictures. These pictures were then compared against a model of a real scene.

4.1. Color Difference Calculations

The color difference calculations involved the computation of tristimulus values for the 24 color swatches in the Macbeth Color Checker chart. The reflectances of these swatches (Figs. 5a to 5g) are representative of commonly occurring reflectances (McCamy, Marcus, and Davidson [15]). CIE standard illuminant C was used as the light source in all of the tests. The color difference between the actual tristimulus values and those determined using various quadrature techniques were expressed as a distance in CIE $L^*a^*b^*$ space [16]. The nominally white object color stimulus was taken to be illuminant C in the computation of the $L^*a^*b^*$ coordinates.

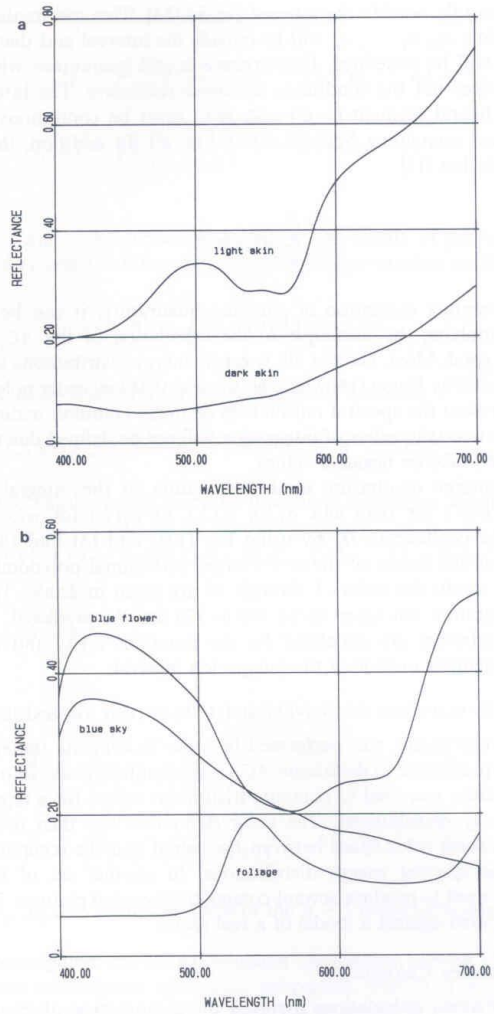

FIG. 5. (a) Reflectances of the light skin and dark skin patches in the Macbeth Color Checker cha (after [15]). (b) Reflectances of the blue flower, blue sky, and foliage patches in the Macbeth Col Checker chart (after [15]). (c) Reflectances of the purple, purplish blue, and bluish green patches in t Macbeth Color Checker chart (after [15]). (d) Reflectances of the blue, green, and red patches in t Macbeth Color Checker chart (after [15]). (e) Reflectances of the cyan, yellow, and magenta patches the Macbeth Color Checker chart (after [15]). (f) Reflectances of the yellow green, orange yellow, oran and moderate red patches in the Macbeth Color Checker chart (after [15]). (g) Reflectances of the whi neutral 8, neutral 6.5, neutral 5, neutral 3.5, and black patches in the Macbeth Color Checker chart (af [15]).

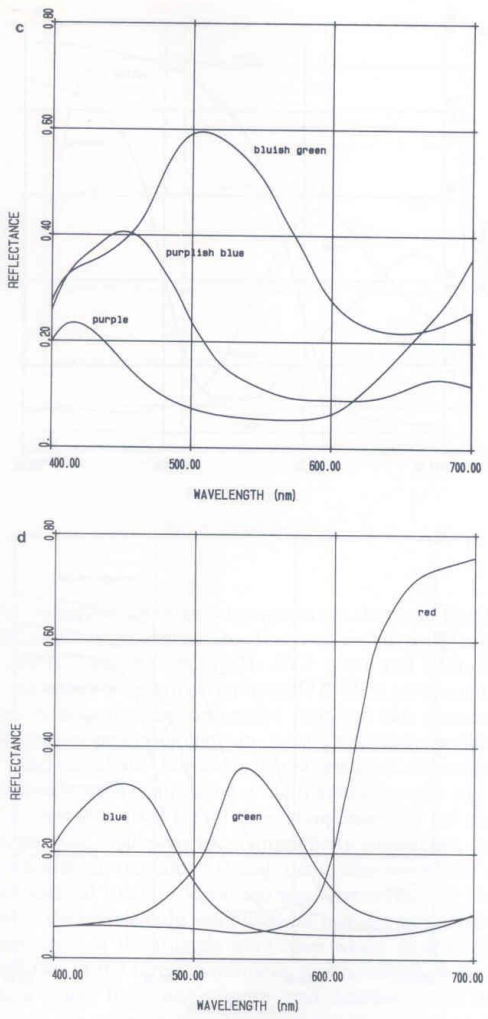

FIG. 5.—*Continued.*

The first test compared gaussian quadrature performed in the AC_1C_2 space defined by Eq. (9) against gaussian quadrature performed in CIE XYZ space and against gaussian quadrature performed in SML space defined by Eq. (1). The wavelengths and coefficients used to compute the AC_1C_2 tristimulus values are given in Tables 1a and 1b. For CIE XYZ space and SML space, the gaussian wavelengths and coefficients were computed by using Eqs. (13) and (16a). For each color space

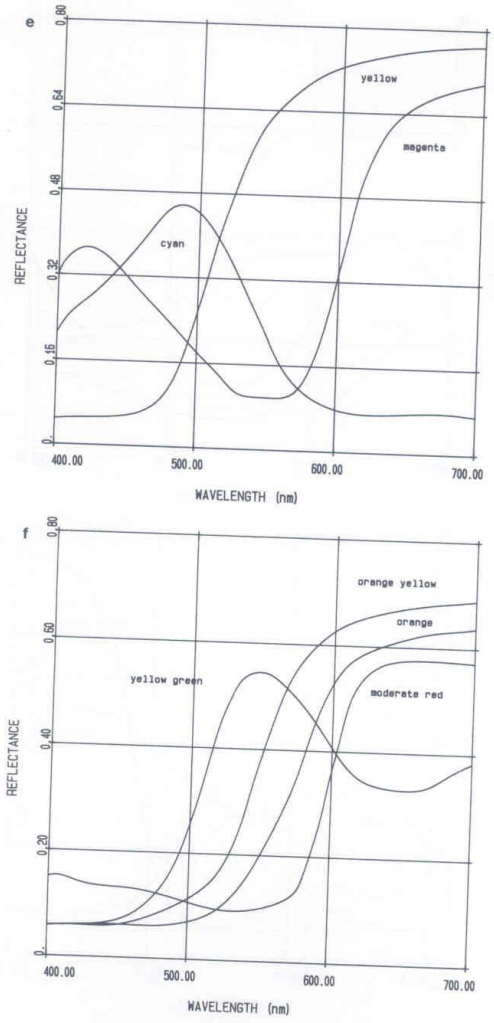

FIG. 5.—*Continued.*

the average color error per patch of the Macbeth Color Checker chart w determined for every possible combination of integration order. The results fr those combinations which employed the same total number of wavelengths we then averaged. This was done to eliminate the importance of any one of t components of a tristimulus value and to accommodate the fact that certa combinations of integration order for *SML* and CIE *XYZ* space are undefined f

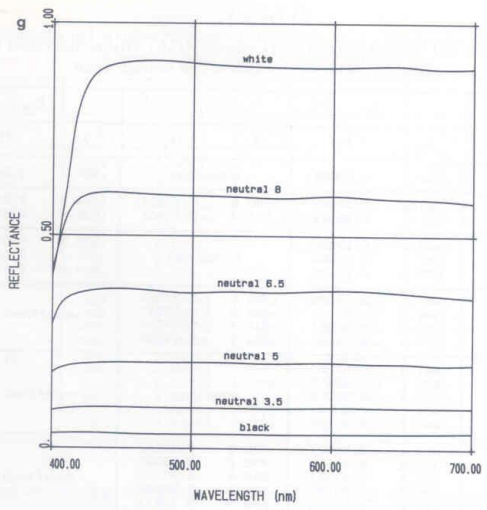

FIG. 5.—*Continued.*

AC_1C_2 space. The results for the three color spaces are shown in Fig. 6. At each level of computational expense as defined by the number of wavelengths employed, AC_1C_2 space is clearly superior to both CIE *XYZ* space and *SML* space.

The next test evaluated the relative importance of each component of the AC_1C_2 tristimulus values. A diagram was constructed from the data obtained by using all possible combinations of orders to compute AC_1C_2 tristimulus values for the color patches of the Macbeth chart. For each combination of orders, the number of wavelengths allocated to each component of the tristimulus value was divided by the total number of wavelengths used for all three components of the tristimulus value. This produced a fraction, analogous to a chromaticity coordinate, for each component. The three wavelength fractions for each data point were used to determine a position on an equilateral triangle. Locations near the corners of the triangle were cases where most of the wavelengths were used for just one of the three coordinates, positions near the edges of the triangle were cases where most of the wavelengths were used for just two of the three coordinates, and positions in the interior of the triangle were cases where there was a more even distribution of the wavelengths among all three of the coordinates. The triangle was discretized into smaller equilateral triangles and an average error, expressed as a distance in $L^*a^*b^*$ space, was computed for each subtriangle from the data points that fell within the subtriangle's boundaries. This average error determined the height of a triangular bar positioned above the subtriangle.

The diagram that results from the above procedure is shown in Fig. 7. Clearly the best results occur in the interior portions of the diagram where the wavelengths are distributed among all of the coordinates. However, in cases where more wavelengths are used for one coordinate than for the other two, smaller errors occur when the A coordinate is favored over the C_1 and C_2 coordinates. To a lesser extent, the C_1

TABLE 1a
Wavelengths and Weights Necessary to Compute AC_1C_2 Tristimulus Values Using Gaussian Quadrature of Orders One through Eight

order	A		C_1		C_2	
	λ_i	H_i	λ_i	H_i	λ_i	H_i
1	559.2	1.05638	undefined		456.4	0.54640
2	516.9 601.5	0.52827 0.52811	490.9 631.4	0.31824 −0.46008	444.0 631.6	0.51004 0.03636
3	483.0 557.7 632.3	0.15908 0.71695 0.18035	undefined		386.9 447.7 644.9	0.01859 0.49780 0.03001
4	457.6 529.3 592.5 660.5	0.04639 0.50400 0.46254 0.04346	450.8 509.9 618.4 679.3	0.04863 0.33007 −0.47764 −0.04290	undefined	
5	441.3 506.7 562.3 621.0 688.4	0.01727 0.25935 0.56306 0.20904 0.00766	undefined		undefined	
6	429.4 484.6 537.8 590.4 644.8 713.4	0.00697 0.10576 0.47284 0.39430 0.07519 0.00131	428.3 468.2 518.5 610.9 658.3 723.6	0.00607 0.08951 0.30806 −0.43681 −0.10674 −0.00193	undefined	
7	419.1 465.0 517.7 564.7 614.0 665.6 732.0	0.00261 0.04337 0.30092 0.47041 0.21567 0.02311 0.00030	undefined		401.2 433.3 466.4 546.5 618.3 664.7 729.5	0.01622 0.25009 0.27643 −0.04131 0.03706 0.00779 0.00013
8	409.6 450.0 499.3 543.0 588.1 634.2 684.4 744.4	0.00089 0.02039 0.15315 0.42595 0.34893 0.10036 0.00662 0.00010	407.3 443.1 481.0 524.3 605.5 645.7 693.1 748.3	0.00031 0.02106 0.11686 0.28008 −0.38470 −0.16389 −0.01134 −0.00022	undefined	

coordinate is also to be preferred over the C_2 coordinate. These results consistent with the prediction of the eigenvalue ratio given in Eq. (10).

The final test explored one specific approach to keeping the total number wavelengths employed to an absolute minimum. This approach is based on assumption that no matter how many wavelengths are used, one wavelength each of the major peaks in the $\bar{a}(\lambda)$, $\bar{c}_1(\lambda)$, and $\bar{c}_2(\lambda)$ functions in Fig. 4 should correctly determined. First-order quadrature for the C_2 component and second-or quadrature for the C_1 component requires the three wavelengths and weights gi in Table 1a. This takes care of three of the major peaks and distributes wavelengths between the C_1 and C_2 components in a manner consistent with eigenvalue ratio and the results of the last test. Third-order quadrature for the component takes care of the fourth major peak and allocates the most waveleng to the most important coordinate. The first row in Table 2 repeats from Table 1a wavelengths and weights necessary to perform gaussian quadrature with this com nation of orders. Also given is the average error in $L^*a^*b^*$ space when tristimulus values of the Macbeth Color Checker chart are computed using th parameters.

TABLE 1b

Wavelengths and Weights Necessary to Compute AC_1C_2 Tristimulus Values Using Gaussian Quadrature of Orders Nine and Ten

order	A		C_1		C_2	
	λ_i	H_i	λ_i	H_i	λ_i	H_i
9	401.6	0.00031	undefined		390.6	0.00309
	439.0	0.01036			419.2	0.08580
	482.0	0.07168			444.1	0.27309
	525.0	0.31122			473.2	0.18523
	566.1	0.40479			543.1	-0.04554
	608.6	0.21487			616.0	0.03344
	651.8	0.04113			654.9	0.01064
	700.9	0.00199			701.9	0.00063
	752.5	0.00004			752.5	0.00001
10	395.6	0.00013	389.9	0.00001	389.1	0.00234
	430.7	0.00542	426.3	0.00367	416.8	0.06757
	467.5	0.03658	455.9	0.04038	441.5	0.26510
	509.3	0.18889	491.7	0.13564	470.8	0.20992
	547.0	0.38063	528.8	0.24852	548.1	-0.05047
	586.4	0.31151	601.2	-0.33288	580.7	0.01304
	626.4	0.11678	636.4	-0.20508	623.2	0.03172
	667.6	0.01572	674.8	-0.03047	663.3	0.00685
	714.4	0.00070	719.2	-0.00156	710.4	0.00033
	757.7	0.00002	759.2	-0.00006	756.2	0.00001

Comparison of the wavelengths used for third-order quadrature of the A component and second-order quadrature of the C_1 component reveals that the two wavelengths used for the C_1 component are very close to two of the wavelengths used for the A component. If the two wavelengths from the C_1 component are substituted for those of the A component, new coefficients for the A component can be determined by use of Eq. (13). The results are given in the second row of Table 2

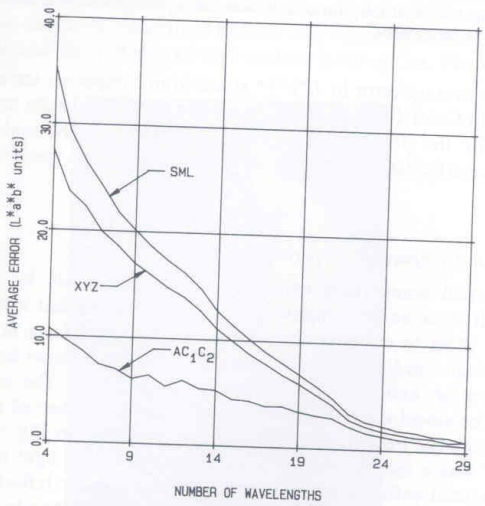

FIG. 6. Average error produced when using gaussian quadrature in three different color spaces to compute tristimulus values for Macbeth Color Checker chart.

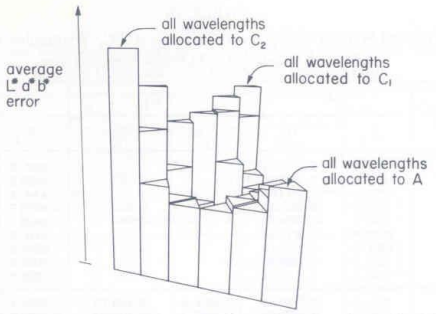

FIG. 7. Average $L^*a^*b^*$ error verses fraction of wavelengths allocated to the calculation of tristimulus value component. Results obtained using the Macbeth Color Checker chart.

TABLE 2

Results from Using Gaussian Quadrature to Compute the Tristimulus Values of the Macbeth Color Checker Chart

A		C_1		C_2		$L^*a^*b^*$ error
λ_i	H_i	λ_i	H_i	λ_i	H_i	
483.0	0.15908	490.9	0.31824	456.4	0.54640	5.432
557.7	0.71695	631.4	−0.46008			
632.3	0.18035					
490.9	0.18892	490.9	0.31824	456.4	0.54640	5.429
557.7	0.67493	631.4	−0.46008			
631.4	0.19253					

Note. In the second row, wavelengths from the C_1 component have also been used for the A component.

along with the average error in $L^*a^*b^*$ space from computing the tristimulus va of the Macbeth Color Checker chart. As can be seen, the results are even a littl better than for the previous case. These four wavelengths and their associ weights are a particularly efficient combination for use in synthetic image gen tion.

4.2. *Perceptual Comparison Experiment*

The perceptual comparison experiment involved a side by side compari between a real scene and a computer generated picture of that scene. This was p of a broader effort to evaluate computer graphic images from both a radiome and a perceptual standpoint (Meyer *et al.* [17]). Figure 8 shows how the model, television monitor, and the view cameras were arranged. The subjects were s arated from the model and the monitor by a curtain and observed the model and monitor through the backs of the view cameras as shown in Fig. 9.

The model was a simple cube with one open side and a light in the ceiling. walls were painted with flat white latex housepaint and the reflectance of the p was measured. Illumination was provided by a tungsten light which shined thro a piece of opal glass. The spectral energy distribution of the light source was measured with a spectrophotometer. A small flap was placed on the front of the

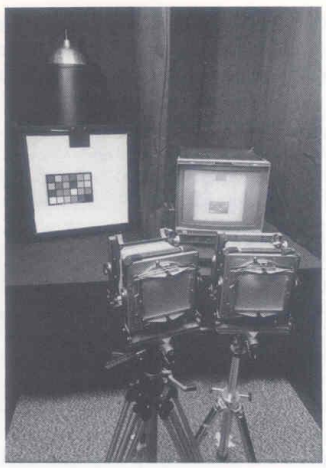

FIG. 8. Experimental setup with partioning curtains removed.

to obscure the light when the box was viewed from the front. This minimized the range of light intensities present in the scene.

The radiosity method (Goral *et al.* [18], Cohen and Greenberg [19]) was used to produce the computer generated pictures. This technique is based on the assumption that the environment can be discretized and that each of the surfaces either emits or reflects in a pure diffuse (Lambertian) manner. An energy balance is performed on the environment and the radiosity of each surface is solved for. The calculations are

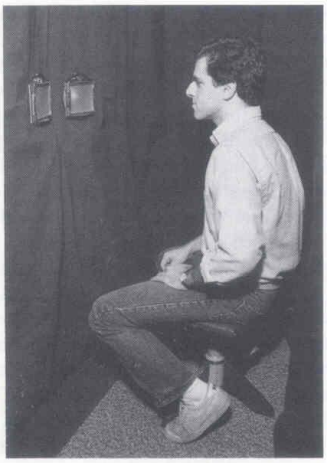

FIG. 9. Subject comparing the real and simulated images.

performed on a wavelength basis. The resulting spectral energy distributions a resolved to tristimulus values and are displayed on a color television monitor.

The monitor had a 20-inch display tube with phosphor chromaticity coordinat

$$x_r = 0.64 \qquad x_g = 0.29 \qquad x_b = 0.15$$

$$y_r = 0.33 \qquad y_g = 0.60 \qquad y_b = 0.06. \qquad (1$$

The individual brightness and contrast controls for each of the monitor guns we adjusted to yield a D6500 white point, and the individual gamma correcti functions were measured for each of the guns. (The curves that were measured we used as is with no attempt to fit them with a single power law curve.) The luminan ratios necessary to set the white point were found to be:

$$Y_r : Y_g : Y_b = 102.4 : 2.29 : 0.0221. \qquad (1$$

By determining the proportional relationship between luminance and radiance f each of the guns, these luminance ratios were converted to radiance ratios and we used to balance the guns over their entire dynamic range. The luminance of t white point was set to 24 foot lamberts.

Two 4 × 5 view cameras were used to view the model and the monitor. Fresn lenses were placed in front of the ground glass of each camera to act as ima intensifiers. The combination of *f*-stop setting and camera to model distance we such that the entire depth of the model was in focus, thereby minimizing depth field problems. The images, as seen by the subjects, were inverted.

The images were computed with the frustum angle and the eye point positi selected to properly simulate the view camera's optics. Two of the images to compared were computed using two different sets of matching functions: *SM* human fundamentals (Eq. (1)) and the optimal AC_1C_2 set based on a transform the human fundamentals (Eq. (9)). First-order gaussian quadrature was used for t synthesis of each image. The resulting tristimulus values were converted to C *XYZ* coordinates. Two other images to be compared were both computed using t AC_1C_2 matching functions. In this case, one of the images used zeroeth-ord gaussian quadrature for the *A* fundamental and third-order gaussian quadrature f the C_1 fundamental while the other image used second-order gaussian quadratu for the *A* fundamental and first-order gaussian quadrature for the C_1 fundament Zeroeth-order gaussian quadrature was used for the C_2 fundamental of each imag The wavelengths and weights used are given in Table 1a. The resulting tristimul values were converted to CIE *XYZ* coordinates. One image to be evaluated w computed using the AC_1C_2 set of matching functions but using only a total of fo wavelengths. The wavelengths and weights used are given in Table 2. CIE *XY* coordinates were found from the tristimulus values. In all cases, *RGB* triplets we found by applying a matrix based on the chromaticity coordinates of the monit phosphors and the monitor white point [20, 21]. These *RGB* triplets were subs quently gamma corrected and loaded into the frame store.

The subjects for the test consisted of 16 members of the Cornell Universit Program of Computer Graphics Lab who had extensive experience evaluati

computer graphic images. In order to factor out the possible effect of order of presentation, 10 of the group were shown the comparison images in AB order and 6 of the group were shown them in BA order. All of the subjects had normal color vision as determined by use of the Ishihara plates.

The questionnaire used in this experiment can be found in Appendix B. It consisted of a brief set of instructions and a series of three questions. For the test the subjects were told that the real model was on the left and the computer generated image was on the right. Two of the questions involved A/B comparisons between the members of the two pairs of images described above. A third question asked for a rating of the color match between the real model and the image computed using only four wavelengths.

In addition to the instructions on the questionnaire each subject was also given some verbal instructions before taking the test. First the chair was adjusted so that each person's head was in roughly the same position. Then they were told not to lean forward to get closer to the view cameras or to turn their head from side to side. All evaluations were to be made by shifting the gaze from one view camera to another.

The results of the experiment are given in Table 3. When the images were computed using different fundamentals but the same number of wavelengths for each component of the tristimulus values, the subjects showed a clear preference for the image produced using the AC_1C_2 fundamentals over the image produced using the SML fundamentals. The sign test indicates that this result is significant at the 0.05 confidence level. The order of presentation of the two images can be shown by Fisher's exact test to have had no significant effect. When the AC_1C_2 fundamentals were used to compute the tristimulus values for each image but the number of wavelengths allocated for each AC_1C_2 component was varied, the image where more wavelengths were allocated to A was clearly preferred to the image where more wavelengths were allocated to C_1. Once again, the sign test indicates that this result is significant at the 0.05 confidence level while Fisher's exact test shows that the

TABLE 3
Results from Perceptual Comparison Experiment

QUESTION	TOTAL	ORDER OF PRESENTATION	
2. Compare AC_1C_2 with SML (% that selected AC_1C_2)	81.25	AC_1C_2 then SML (6 subjects)	SML then AC_1C_2 (10 subjects)
		83.33	80.00
3. Compare more wavelengths for A with more wavelengths for C_1 (% that chose more wavelengths for A)	87.50	A then C_1 (10 subjects)	C_1 then A (6 subjects)
		80.00	100.00
1. Rate the color match for four wavelength AC_1C_2 (mean score)	3.06		

order of presentation had no significant effect. Finally, the color match between th real model and the image computed using the AC_1C_2 fundamentals and a total four wavelengths was rated as being good.

5. SUMMARY AND CONCLUSIONS

This paper has shown how gaussian quadrature can be used with a set opponent fundamentals to select the wavelengths at which to perform synthet image generation. The fundamental human spectral sensitivity functions we introduced and were expressed in terms of the CIE XYZ matching functions. Th Karhunen–Loeve expansion was used to transform these functions into a set opponent fundamentals. Gaussian quadrature with the opponent fundamentals weighting functions was used to select wavelengths for realistic image synthesis. Th spectral reflectances of the Macbeth Color Checker chart were used to evaluate th technique. This was accomplished through color difference calculations and perceptual comparison experiment.

It can be concluded that an opponent color space, such as AC_1C_2 space, ha important properties for realistic image synthesis. Better color accuracy is achieve with fewer wavelengths when the wavelengths are selected based on AC_1C_2 spac than when they are chosen using either CIE XYZ space or SML space. Withi AC_1C_2 space itself, the A coordinate is most important, the C_1 coordinate is secon most important, and the C_2 coordinate is least important. This information can b used to select wavelengths for synthetic image generation and leads to a particularl efficient four wavelength set that roughly corresponds to the four peaks of th opponent fundamentals themselves.

The primary area for future work is to extend the wavelength selection technique to discontinuous spectral energy distributions. This would avoid the situation where the peaks of a "spikey" spectral energy distribution lie between the wavelength selected to perform the simulation. Some type of prefiltering of the spectral energy distribution should overcome this problem.

APPENDIX A: DERIVATION OF THE FUNDAMENTAL SPECTRAL SENSITIVITIES

This appendix derives the fundamental spectral sensitivity functions that are use in this paper. In order for this derivation to proceed, the dichromatic chromaticity confusion loci must be known and the relative sensitivity of the resulting function must be established. Once these things are known, the fundamental spectra sensitivity functions can be expressed in terms of the 1931 CIE standard observe color matching functions $\bar{x}(\lambda)$, $\bar{y}(\lambda)$, and $\bar{z}(\lambda)$.

The chromaticity confusion loci are the points where the axes of the color spac corresponding to the actual human spectral sensitivity functions penetrate the 193 CIE XYZ chromaticity diagram. From the many possible alternatives, the loc proposed by Estevez [22] have been selected. The suggested protanopic, deuter- anopic, and tritanopic confusion loci are:

$$\begin{aligned} x_p &= 0.735 \quad x_d = 1.14 \quad x_t = 0.171 \\ y_p &= 0.265 \quad y_d = -0.14 \quad y_t = -0.003. \end{aligned} \tag{20}$$

The Estevez [22] study was used because it was the only one that considered all three loci simultaneously with the express intention of defining a set of fundamental spectral sensitivities. (In order to avoid negative values for the fundamentals, $x_p = 0.735$ was used for the protanopic confusion point instead of the $x_p = 0.73$ recommended in Estevez [22]. y_p was found from the relation $y_p = 1.0 - x_p$.) When the 1931 CIE standard observer color matching functions are transformed into the color space defined by these loci, three fundamental spectral sensitivities emerge which peak at approximately 446, 543, and 560 nm (Fig. 1). They will be referred to as the short ($\bar{s}(\lambda)$), medium ($\bar{m}(\lambda)$), and long ($\bar{l}(\lambda)$) wavelength sensitivities.

The relative sensitivities of the three functions in Fig. 1 were determined by employing a technique developed by Vos and Walraven [23] and Walraven [24]. Based primarily on the assumption that the nerve signals must be balanced in order for hue to remain constant with intensity at wavelengths 475.5 nm and 570 nm, and the assumption that the neural network which produces these signals has an opponents architecture, it is postulated in these articles that the following relations must hold for the fundamental spectral sensitivities $\bar{s}(\lambda)$, $\bar{m}(\lambda)$, and $\bar{l}(\lambda)$:

$$\frac{\bar{s}(475.5)}{\bar{m}(475.5) + \bar{l}(475.5)} = \frac{1}{16}$$
$$\frac{\bar{l}(570.0)}{\bar{m}(570.0)} = 2. \tag{21}$$

This is shown to imply that the foveal cone receptors have effective population densities in the ratios $L : M : S := 32 : 16 : 1$. This correlates nicely with a receptor mosaic which has been shown to be hexagonal in pattern.

Given the 1931 CIE standard observer matching functions, the dichromatic chromaticity confusion loci in Eq. (20), and the ratios of Eq. (21), the definition of the fundamental spectral sensitivities given in Eq. (1) can be derived as shown in Wyszecki and Stiles [25]. It is important to note that there are limitations to the accuracy of the 1931 CIE standard observer and that there are alternative color matching data available. The accuracy of the data was limited because brightness matching had to be substituted for radiometric measurements due to the limitations of the technology available in 1931. There have also been corrections to the photopic luminous efficiency function since that time which would change the definition of the standard observer's $\bar{y}(\lambda)$ matching function. In 1952, Stiles and Burch [26, 27] used modern instrumentation to perform the color matching experiments again. Estevez [22] has recommended the use of these color matching functions in lieu of the 1931 CIE standard observer. However, in this paper the standard observer data is employed because certain colorimetric data (like the chromaticity coordinates of phosphors) is only expressed in terms of the 1931 CIE standard observer.

APPENDIX B: Perceptual Comparison Experiment Questionnaire

The tests to which these questions pertain will be administered by the experimenter who is in the room with you. You will be told when to answer each of the questions. Please put the questionnaire in the box when you are done. Your responses will remain anonymous.

1. How well do the colors in the computer generated picture on the right mat the colors in the picture of the actual model on the left?

(a) excellent
(b) good
(c) fair
(d) poor
(e) bad

2. In which of the two computer generated pictures are the colors a better mat to the colors in the picture of the actual model?

(a)
(b)

3. In which of the two computer generated pictures are the colors a better mat to the colors in the picture of the actual model?

(a)
(b)

ACKNOWLEDGMENTS

Professor Donald P. Greenberg supervised this research from its inception. Hel in performing the statistical analysis was provided by Professor Thomas Gilovich Holly Rushmeier and Michael Cohen helped construct the equipment for th comparison experiment and assisted in conducting the tests that were involved Michael also wrote the radiosity software that was used to produce the pictures tha were used in these experiments. This work was performed under partial funding b National Science Foundation grant DCR-8203979, "Interactive Computer Graphic Input and Display Techniques."

REFERENCES

1. R. L. Cook and K. E. Torrance, A reflectance model for computer graphics, *ACM Trans. Graphics* 1982, 7–24.
2. R. A. Hall and D. P. Greenberg, A testbed for realistic image synthesis, *IEEE Comput. Graphic Appl.* **3**, 1983, 10–20.
3. G. Buchsbaum and A. Gottschalk, Trichromacy, opponent colours coding and optimum colou information transmission in the retina, *Proc. R. Soc. London Ser. B*, **220**, 1983, 89–113.
4. A. Gottschalk and G. Buchsbaum, Information theoretic aspects of color signal processing in th visual system, *IEEE Trans. Systems Man Cybernet.*, **SMC-13**, 1983, 864–873.
5. K. Fukunaga, *Introduction to Statistical Pattern Recognition*, Academic Press, New York, 1972.
6. D. Middleton, *An Introduction to Statistical Communication Theory*, McGraw–Hill, New York, 196
7. C. R. Ingling, The spectral sensitivity of the opponent-color channels, *Vision Res.* **17**, 197 1083–1089.
8. S. L. Guth, R. W. Massof, and T. Benzschawel, Vector model of normal and dichromatic colo vision, *J. Opt. Soc. Amer.* **70**, 1980, 197–212.
9. R. Wallis, Fast computation of tristimulus values by use of gaussian quadrature, *J. Opt. Soc. Amer* **65**, 1975, 542–545.
10. D. L. MacAdam, *Color Measurement: Theme and Variations*, Springer-Verlag, Berlin, 1981.
11. S. D. Conte and C. deBoor, *Elementary Numerical Analysis: An Algorithmic Approach*, 2nd ed. McGraw–Hill, New York, 1972.

12. P. J. Davis and P. Rabinowitz, *Methods of Numerical Integration*, Academic Press, New York, 1975.
13. A. H. Stroud and D. Secrest, *Gaussian Quadrature Formulas*, Prentice–Hall, Englewood Cliffs, NJ, 1966.
14. P. Moon, Polynomial representation of reflectance curves, *J. Opt. Soc. Amer.* **35**, 1945, 597–600.
15. C. S. McCamy, H. Marcus, and J. G. Davidson, A color-rendition chart, *J. Appl. Photogr. Eng.* **2**, 1976, 95–99.
16. CIE recommendations on uniform color spaces, color-difference equations, and psychometric color terms, Supplement No. 2 to Publication CIE No. 15, *Colorimetry* (E-1.3.1) 1971, Bureau Central de la CIE, Paris, 1978.
17. G. W. Meyer, H. E. Rushmeier, M. F. Cohen, D. P. Greenberg, and K. E. Torrance, An experimental evaluation of computer graphics imagery, *ACM Trans. Graphics* **5**, 1986, 30–50.
18. C. Goral, K. E. Torrance, D. P. Greenberg, and B. Battaile, Modeling the interaction of light between diffuse surfaces, *Comput. Graphics* **18**, 1984, 213–222.
19. M. Cohen and D. P. Greenberg, The hemi-cube: A radiosity solution for complex environments, *Comput. Graphics* **19**, 1985, 31–40.
20. W. B. Cowan, An inexpensive scheme for calibration of a colour monitor in terms of the CIE standard coordinates, *Comput. Graphics* **17**, 1983, 315–321.
21. G. Meyer and D. P. Greenberg, Perceptual color spaces for computer graphics, *Comput. Graphics* **14**, 1980, 254–261.
22. O. Estevez, *On the Fundamental Data-Base of Normal and Dichromatic Color Vision*, Ph.D. thesis, University of Amsterdam, 1979.
23. J. J. Vos and P. L. Walraven, On the derivation of the foveal receptor primaries, *Vision Res.* **11**, 1970, 799–818.
24. P. L. Walraven. A closer look at the tritanopic convergence point, *Vision Res.* **14**, 1974, 1339–1343.
25. G. Wyszecki and W. S. Stiles, *Color Science: Concepts and Methods, Quantitative Data and Formulae*, 2nd ed., Wiley, New York, 1982.
26. W. S. Stiles and J. M. Burch, Interim report to the Commission Internationale de l'Eclairage, Zurich, 1955, on the National Physical Laboratory's investigation of colormatching, *Opt. Acta*, **2**, 1955, 168.
27. W. S. Stiles and J. M. Burch, N.P.L. colour-matching investigation: Final report (1958), *Opt. Acta* **6**, 1959, 1.